

ON LINEARIZED COUPLING CONDITIONS FOR A CLASS OF ISENTROPIC MULTIPHASE DRIFT-FLUX MODELS AT PIPE-TO-PIPE INTERSECTIONS

MAPUNDI K. BANDA¹, MICHAEL HERTY² AND JEAN MEDARD T. NGNOTCHOUYE³

ABSTRACT. In this paper a general drift-flux model describing a subsonic and isentropic multi-phase fluid in connected pipes is considered. Each phase is assumed to be isentropic with its own sonic speed. The components are gamma-law gases with $\gamma > 1$. For such the computational challenge at a junction is the computation of rarefaction waves which do not have a readily available analytical form. Firstly, the well-posedness of the Riemann problem at the junction is discussed. It is suggested that rarefaction waves should be linearized in order to obtain a more efficient numerical method for coupling such multi-component flow. Some computational results on the dynamics of the multi-phase gas in the pipes demonstrate the qualitative behaviour of this approach.

Key Words: Drift-flux model, multiphase flows, network flow, systems of conservation laws.

1. INTRODUCTION

The isothermal no-slip drift flux model for multiphase flow in a network of pipes can be represented in the form

$$(1) \quad \begin{aligned} \partial_t \rho_1 + \partial_x \rho_1 u &= 0 \\ \partial_t \rho_2 + \partial_x \rho_2 u &= 0 \\ \partial_t (\rho_1 u + \rho_2 u) + \partial_x ((\rho_1 + \rho_2)u^2 + p(\rho_1, \rho_2)) &= 0 \end{aligned}$$

where ρ_1 and ρ_2 are the density of phase 1 and 2, respectively, u is the common velocity and $p = p(\rho_1, \rho_2)$ is the pressure. The two fluids are assumed to be immiscible and, therefore, denote the density of each component as $\rho_1 = \alpha_1 \varrho_1$ and $\rho_2 = \alpha_2 \varrho_2$ with $\alpha_1 + \alpha_2 = 1$ where α_1 and α_2 are the volume fractions of each phase and ϱ_1, ϱ_2 are the phase densities. This flow model is derived from the *two-fluid* model by averaging the balance law for the momentum in the canonical form.

In this paper, the flow of a class of isentropic drift-flux models (1) in a pipe-to-pipe intersection is investigated. Here, every connected pipe is viewed as an arc oriented by parameterization. The focus is on coupling conditions for (1) with a *general pressure law* especially at the junctions of a network giving rise to suitable boundary conditions for the pipes intersecting at a junction where extra conditions are defined for the evolution of the flow solution in the network. A similar study for $p(\rho_1, \rho_2) = a^2(\rho_1 + \rho_2)$ has been conducted in [3] and for $p(\rho_1, \rho_2) = a_1^2 \rho_1 + a_2^2 \rho_2$ in [4]. We present a theoretical as well as a computational treatment of the general case (with numerical examples for a γ -law) giving rise to the numerical problems of not having an explicit formula for the wave curves. To overcome this difficulty and to obtain an efficient numerical integration at the pipe-to-pipe intersection, we linearize the wave curves and solve the coupling conditions on the linearized wave curves. This is the main contribution of this paper. Numerical tests are undertaken which justify this approach. Comparisons are also done with a standard solver. The results compare favourably. As expected, application of the approach to isentropic models gives very good results.

¹Department of Mathematics and Applied Mathematics, University of Pretoria, Private Bag X20, Hatfield 0028, South Africa (mapundi.banda@up.ac.za).

²RWTH Aachen, IGPM, Templergraben 55, D-52056 Aachen, Germany (herty@igpm.rwth-aachen.de).

³School of Mathematics, Statistics and Computer Science, University of KwaZulu-Natal, Private Bag X01, Scottsville 3209, South Africa (ngnotchouye@ukzn.ac.za).

The mathematical study of flow of fluid in networks of pipes is a very active field of research. The interested reader may refer to [1, 2, 6, 7, 12] for the case of gas networks, to [21, 25] for water networks and [19, 24] for traffic networks. These models consider single phase flow. The study of the multiphase case has been introduced in [3, 4] for some special drift-flux models where the pressure law was taken as a linear function of the densities allowing for an explicit computation of the wave curves.

The rest of the paper is organized as follows. In Section 2, a brief discussion of the derivation of the flow model is presented. A solution of the standard Riemann problem is given. A mathematical analysis for a junction of pipes in a network is considered in Section 3. A rigorous definition of the Riemann problem at the junction is given including precise coupling conditions. The well-posedness of the Riemann problem at a junction of two connected pipes is presented. The general case of a junction with m ingoing pipes and p outgoing pipes is briefly discussed. Section 4 is devoted to some numerical simulations and results. The effect of the sound speed of the two phases on the junction is investigated. Thereafter the numerical results of the linearization of the Lax curves are presented. Applications of this approach for solving the Riemann problem at the junction of three connected pipes as well as a small network are also presented. A conclusion and ideas for further work are presented in Section 5.

2. MODEL FORMULATION AND PRELIMINARY RESULTS

A mixture of two fluids with density, volume fraction, velocity and pressure denoted by ϱ_i , α_i , u_i , p_i , respectively, for $i = 1, 2$ is considered. A common model for such multiphase fluid is the drift-flux model [14] which takes the form presented in Equation (1). As in [15], we assume that the pressure and the velocity of the two components are equal. A pressure law $p(\rho_1, \rho_2)$ can be derived as follows: For each component the pressure in this case has the form $p = \hat{\kappa}\rho^\gamma \equiv P(\rho)$ where $\hat{\kappa} \geq 0$ and $\gamma > 1$ are constants. Physically, $P'(\rho) > 0$ for $\rho > 0$. Hence for each phase the pressure takes the form

$$(2) \quad p = p_i(\varrho_i) = a_i^2 \varrho_i^\gamma, \quad i \in \{1, 2\},$$

where the positive constant a_i is the compressibility factor or sound speed of phase i . The relation $\alpha_1 + \alpha_2 = 1$ can then be written as

$$\frac{\rho_1}{\varrho_1} + \frac{\rho_2}{\varrho_2} = \frac{\rho_1}{\left(p/a_1^2\right)^{1/\gamma}} + \frac{\rho_2}{\left(p/a_2^2\right)^{1/\gamma}} = 1.$$

Hence,

$$(3) \quad p(\rho_1, \rho_2) = (\rho_1 a_1^{2/\gamma} + \rho_2 a_2^{2/\gamma})^\gamma.$$

Clearly, the expression simplifies to the ones studied in [3, 4] when the two fluids have the same compressibility factors, $a_1 = a_2 = a$:

$$(4) \quad p(\rho_1, \rho_2) = a^2(\rho_1 + \rho_2)^\gamma.$$

For a mathematical study, the following reformulation of the model is advantageous. Introduce the total momentum and densities

$$I = \hat{\rho}u \quad \text{and} \quad \hat{\rho} = \rho_1 + \rho_2,$$

respectively. Then, (1) is equivalent to the following equation in conservative variables (ρ_1, ρ_2, I) and unspecified pressure $p = p(\rho_1, \rho_2)$

$$(5) \quad \begin{aligned} \partial_t \rho_1 + \partial_x \frac{\rho_1 I}{\hat{\rho}} &= 0; \\ \partial_t \rho_2 + \partial_x \frac{\rho_2 I}{\hat{\rho}} &= 0; \\ \partial_t I + \partial_x \left(\frac{I^2}{\hat{\rho}} + p \right) &= 0. \end{aligned}$$

Before discussing in details the dynamics at a pipe-to-pipe intersection, the solutions of the standard Riemann problem for Equation (5) are presented. Those will be used later in the construction of solutions to the coupled problem. As it is well known [13], the exact solution to a Riemann problem is constructed as a set of constant states connected by wave curves.

The equation of state $p = p(\rho_1, \rho_2)$ is considered as general as possible and depends on the density of each phase. Later, for illustration and numerical purposes, the isentropic model (3) is used.

For brevity, the following notations for the partial derivatives of $p(\rho_1, \rho_2)$ are introduced:

$$p_1 = \frac{\partial p}{\partial \rho_1}, \quad p_2 = \frac{\partial p}{\partial \rho_2}, \quad p_{11} = \frac{\partial^2 p}{\partial \rho_1^2}, \quad p_{22} = \frac{\partial^2 p}{\partial \rho_2^2}, \quad p_{12} = \frac{\partial^2 p}{\partial \rho_1 \partial \rho_2}.$$

The eigenvalues $\lambda_{1,2,3}$ and the eigenvectors $r_{1,2,3}$ of the Jacobian matrix of the flux function of the drift-flux model (5) are given by

$$(6) \quad \lambda_{1,3}(w) = \frac{I}{\hat{\rho}} \mp \sqrt{\frac{\rho_1 p_1 + \rho_2 p_2}{\hat{\rho}}} = \frac{I}{\hat{\rho}} \mp \sqrt{\frac{\gamma p}{\hat{\rho}}}, \quad \lambda_2(w) = \frac{I}{\hat{\rho}},$$

$$r_{1,3}(w) = \begin{bmatrix} \rho_1 \\ \rho_2 \\ \hat{\rho} \lambda_{1,3}(w) \end{bmatrix}, \quad r_2(w) = \begin{bmatrix} p_2 \\ -p_1 \\ (p_2 - p_1) \lambda_2(w) \end{bmatrix}.$$

where $w = [\rho_1, \rho_2, I]^T$ is a vector of conserved variables.

The second field is always linearly degenerate since $\nabla \lambda_2(w) \cdot r_2(w) \equiv 0$. For the fields 1 and 3, one obtains

$$\nabla \lambda_{1,3}(w) \cdot r_{1,3}(w) = \mp \frac{\rho_1^2 p_{11} + \rho_2^2 p_{22} + 2\rho_1 \rho_2 p_{12} + 2(\rho_1 p_1 + \rho_2 p_2)}{2\sqrt{\hat{\rho}(\rho_1 p_1 + \rho_2 p_2)}}.$$

To ensure hyperbolicity and genuine nonlinearity, restrictions need to be applied to the pressure law for which

$$(7) \quad \rho_1 p_1 + \rho_2 p_2 > 0, \quad \forall \rho_1, \rho_2 > 0,$$

and

$$(8) \quad \rho_1^2 p_{11} + \rho_2^2 p_{22} + 2\rho_1 \rho_2 p_{12} + 2(\rho_1 p_1 + \rho_2 p_2) \neq 0.$$

The conditions (7) and (8) are both fulfilled by choosing a pressure law such that

$$(9) \quad p(0, 0) = 0, \quad p_1(\rho_1, \rho_2), \quad p_2(\rho_1, \rho_2) > 0 \quad \text{and} \quad \text{Hess}(p) \quad \text{is positive semi-definite,}$$

where $\text{Hess}(p)$ is the Hessian with respect to (ρ_1, ρ_2) of the map p . Condition (9) is a direct generalization for multi-phase flow of a similar condition for single phase flow, see [6, 12, 17]. Indeed, this condition is fulfilled by the nonlinear pressure law given in (3). Also for a pressure law analogous to (3) with unequal γ 's for each phase, see Appendix A, the same condition is fulfilled. In the following, the Lax-curves, as a preliminary step for the solution of the Riemann problem at the junction, are discussed.

2.1. Shock Curves. The Lax shock curves are derived from the Rankine-Hugoniot jump conditions. Indeed, let w be a given state and assume that another state \bar{w} is connected to w by a 1,3-shock wave of shock speed s . Then w and \bar{w} satisfy

$$(10) \quad f(w) - f(\bar{w}) = s(w - \bar{w}).$$

This system defines a one parameter family of curves found to be

$$(11) \quad S_{1,3}(\xi; w) = (\rho_1 \xi, \rho_2 \xi, I_{1,3}(\xi))^T$$

with

$$(12) \quad I_{1,3}(\xi) = I\xi \mp \sqrt{\hat{\rho}(\xi^2 - \xi)(p(\rho_1\xi, \rho_2\xi) - p(\rho_1, \rho_2))}$$

and the shock speed is given by

$$(13) \quad s_{1,3}(w) = \frac{I}{\hat{\rho}} \mp \frac{\sqrt{\xi(p(\rho_1\xi, \rho_2\xi) - p(\rho_1, \rho_2))}}{\sqrt{\hat{\rho}(\xi - 1)}}.$$

The forward and backward admissible 1-shock curves are obtained, using the Lax admissibility conditions, as $S_1(\xi; w)$ in (12) with $\xi \geq 1$ and $\xi \leq 1$, respectively. Similarly, the forward and backward 3-shock curves are given by $S_3(\xi; w)$ in (12) with $\xi \leq 1$ and $\xi \geq 1$, respectively.

2.2. Contact Discontinuity. Let w and \bar{w} be two given states. Using the linear degeneracy of the second field and the Rankine-Hugoniot jump condition (10), then w belongs to the 2-curve emanating from \bar{w} if

$$w - \bar{w} = \xi r_2(\bar{w}), \quad \xi \in \mathbb{R}.$$

Hence,

$$\begin{aligned} \rho_1 &= \bar{\rho}_1 + \xi \bar{p}_2, \\ \rho_2 &= \bar{\rho}_2 - \xi \bar{p}_1, \\ I &= \bar{I} + \xi(\bar{p}_2 - \bar{p}_1)\lambda_2(\bar{w}). \end{aligned}$$

In the equations above, the notations $\bar{p}_1 = p_1(\bar{\rho}_1, \bar{\rho}_2)$ and $\bar{p}_2 = p_2(\bar{\rho}_1, \bar{\rho}_2)$ are used. Eliminating ξ in this system and after applying suitable scaling, the contact discontinuity wave emanating from any state w is given by the curve

$$(14) \quad L_2(\xi; w) = \frac{1}{p_2} \left[\begin{array}{c} p_2 \rho_1 \xi \\ p_2 \rho_2 - p_1(\xi - 1)\rho_1 \\ \frac{I}{\hat{\rho}} (p_2(\rho_1 + \rho_2) + (p_2 - p_1)\rho_1(\xi - 1)) \end{array} \right].$$

The shock speed is given as

$$s_2(w) = \frac{\frac{I}{\hat{\rho}} (p_2(\rho_1 + \rho_2) + (p_2 - p_1)\rho_1(\xi - 1))}{\rho_1(p_2 - p_1)\xi + \rho_1 p_1 + \rho_2 p_2} = \frac{I}{\rho_1 + \rho_2} = \lambda_2(w).$$

Note that the continuity of pressure along the contact discontinuity is preserved.

2.3. Rarefaction Curves. They are given as integral curves of the eigenvectors of the flux function

$$\frac{dw}{d\xi} = \frac{r_{1,3}(w(\xi))}{\nabla \lambda_{1,3}(w(\xi)) \cdot r_{1,3}(w(\xi))}, \quad \xi \geq \xi_{1,3},$$

with $\xi_{1,3} = \lambda_{1,3}(w)$.

This yields

$$\frac{d}{d\xi} \begin{bmatrix} \rho_1 \\ \rho_2 \\ I \end{bmatrix} = \mp \frac{2\sqrt{\hat{\rho}(\rho_2 p_2 + \rho_1 p_1)}}{\rho_1^2 p_{11} + \rho_2^2 p_{22} + 2\rho_1 \rho_2 p_{12} + 2(\rho_1 p_1 + \rho_2 p_2)} \begin{bmatrix} \rho_1 \\ \rho_2 \\ \hat{\rho} \lambda_{1,3}(w) \end{bmatrix}, \quad \xi \geq \xi_{1,3}.$$

Under the assumptions on the pressure given in (9), the existence of the solution, denoted as $R_{1,3}(\xi; w)$ is proven, for any given state w . For the pressure law given in (3) with $\gamma = 1$, an exact expression for the rarefaction curves was presented in [3].

In general, the forward and backward admissible 1-rarefaction curves for (5) are obtained using the Lax admissibility condition as $R_1(\xi; w)$ with $\xi < 1$, and $\xi > 1$, respectively. Similarly, the forward and backward 3-rarefaction curves are given by $R_3(\xi; w)$ with $\xi > 1$, and $\xi < 1$, respectively. In summary the Lax-curves for the model in Equation (5) are given by

$$(15a) \quad L_1^+(\xi; w) = \begin{cases} S_1(\xi; w), & \xi \geq 1; \\ R_1(\xi; w), & \xi < 1; \end{cases} \quad L_3^+(\xi; w) = \begin{cases} S_3(\xi; w), & \xi \leq 1; \\ R_3(\xi; w), & \xi > 1; \end{cases}$$

$$(15b) \quad L_1^-(\xi; w) = \begin{cases} S_1(\xi; w), & \xi \leq 1; \\ R_1(\xi; w), & \xi > 1; \end{cases} \quad L_3^-(\xi; w) = \begin{cases} S_3(\xi; w), & \xi \geq 1; \\ R_3(\xi; w), & \xi < 1. \end{cases}$$

The Riemann problem for the drift-flux model consists of solving the model Equations (5) with Heaviside-type initial conditions of the form

$$(16) \quad w(x, 0) = \begin{cases} w^+, & \text{if } x > 0; \\ w^-, & \text{if } x < 0. \end{cases}$$

The general theory on the solution of a standard Riemann problem for a system of conservation laws have been presented extensively for example in the books [13, 22, 23]. For completeness and simplicity we present the framework for solving the standard Riemann Problem for $\gamma = 1$ in Appendix A.

3. COUPLING CONDITIONS AT PIPE-TO-PIPE INTERSECTIONS AND THEIR NUMERICAL DISCRETIZATION

In this section and the rest of the paper, the following notation $\mathbb{R}^+ = (0, +\infty)$ and $\overset{\circ}{\mathbb{R}}^+ = [0, +\infty)$ is used. Here the pipe-to-pipe intersections will be studied in which a multiphase flow takes place in *two* connected pipes. The parameterization of the pipes is such that $-\overset{\circ}{\mathbb{R}}^+$ and $\overset{\circ}{\mathbb{R}}^+$ describe the pipes and such that they are coupled at $x = 0$. In the following the coupling conditions will be introduced such that the pipe-to-pipe intersection problem yields consistent solutions compared with a classical Riemann problem.

The flow in each pipe is governed by the drift-flux model equations (5)

$$(17) \quad \partial_t w + \partial_x f(w) = 0, \quad w = \begin{bmatrix} \rho_1 \\ \rho_2 \\ I \end{bmatrix}, \quad f(w) = \begin{bmatrix} \frac{\rho_1 I}{\bar{\rho}} \\ \frac{\rho_2 I}{\bar{\rho}} \\ \frac{I^2}{\bar{\rho}} + p(\rho_1, \rho_2) \end{bmatrix}.$$

At the junction, located at $x = 0$, the dynamics are governed by coupling conditions described by a general possibly nonlinear function

$$\Psi : \mathbb{R}^3 \times \mathbb{R}^3 \rightarrow \mathbb{R}^3$$

and by requiring that any weak solution to (17) also fulfills almost everywhere in time

$$(18) \quad \Psi(w^-(t, 0-); w^+(t, 0+)) = 0,$$

where the w^- and w^+ are the flow variables in the connected pipes, respectively. For constant initial data in each pipe, i.e., for $w(x, 0) = w_0^-$ for $x < 0$ and $w(x, 0) = w_0^+$ for $x > 0$, solutions in the sense of Definition 3.1 to (17) and (18) are constructed under the following assumption

$$(19a) \quad \text{The initial data is assumed to be subsonic, i.e., } w_0^\pm \in A_0$$

$$(19b) \quad \text{and in a neighborhood of a constant state } (\bar{w}^-, \bar{w}^+) \text{ with } \Psi(\bar{w}^-, \bar{w}^+) = 0.$$

Solutions of the Riemann problem at the junction are considered as perturbations of stationary solutions of (5) in the pipes which are intersecting at the junction. The subsonic region defined

as

$$(20) \quad A_0 = \{w \in \overset{\circ}{\mathbb{R}}^+ \times \overset{\circ}{\mathbb{R}}^+ \times \mathbb{R} : \lambda_1(w) < 0 < \lambda_2(w) < \lambda_3(w)\}$$

is considered. We also define the region

$$(21) \quad \tilde{A}_0 := \{w \in \overset{\circ}{\mathbb{R}}^+ \times \overset{\circ}{\mathbb{R}}^+ \times \mathbb{R} : \lambda_1(w) < \lambda_2(w) < 0 < \lambda_3(w)\}$$

which will be used below. Also, for later use, the quantities

$$\begin{aligned} \text{Flow of the density of phase 1:} \quad & M(w) = \frac{\rho_1 I}{\hat{\rho}}, \\ \text{Flow of the density of phase 2:} \quad & N(w) = \frac{\rho_2 I}{\hat{\rho}}, \\ \text{Flow of the linear momentum:} \quad & P(w) = \frac{I^2}{\hat{\rho}} + p(\rho_1, \rho_2) \end{aligned}$$

are defined.

In general, for two connected pipes at a junction, one is interested in Ψ -solutions, that is, weak solutions depending on the coupling conditions map Ψ . A map \hat{w} defined as

$$(22) \quad \hat{w}(x) = \begin{cases} \hat{w}^-, & \text{if } x < 0; \\ \hat{w}^+, & \text{if } x > 0; \end{cases} \quad \text{with} \quad \begin{cases} \Psi(\hat{w}^-; \hat{w}^+) = 0, \\ \hat{w}^-, \hat{w}^+ \in A_0 \end{cases}$$

is considered. The existence of \hat{w} for a given initial condition in a neighborhood of $\bar{w} = (\bar{w}^-, \bar{w}^+)$ has been discussed below. The following definition is a direct extension of [11, Definition 2.2] for the current problem.

Definition 3.1. *A weak Ψ -solution of (5) complemented by (18) is a map*

$$(23) \quad \begin{aligned} w &\in \mathbf{C}^0 \left(\mathbb{R}^+; \hat{w} + \mathbf{L}^1(\mathbb{R}; \overset{\circ}{\mathbb{R}}^+ \times \overset{\circ}{\mathbb{R}}^+ \times \mathbb{R}) \right) \\ w(t) &= w(t, \cdot) \in \mathbf{BV}(\mathbb{R}; \overset{\circ}{\mathbb{R}}^+ \times \overset{\circ}{\mathbb{R}}^+ \times \mathbb{R}) \quad \text{for a.e. } t \in \mathbb{R}^+ \end{aligned}$$

such that

$$(1) \text{ for all } \varphi \in \mathbf{C}_c^1 \left(\overset{\circ}{\mathbb{R}}^+ \times \mathbb{R}; \mathbb{R} \right) \text{ whose support does not intersect } x = 0$$

$$(24) \quad \int_{\mathbb{R}^+} \int_{\mathbb{R}} \left(\begin{bmatrix} \rho_1 \\ \rho_2 \\ I \end{bmatrix} \partial_t \varphi + \begin{bmatrix} M(w) \\ N(w) \\ P(w) \end{bmatrix} \partial_x \varphi \right) dx dt = 0;$$

$$(2) \text{ for a.e. } t \in \mathbb{R}^+, \text{ the junction condition is fulfilled}$$

$$\Psi(w^-(t, 0-); w^+(t, 0+)) = 0.$$

In addition, in order for the solutions to be entropy admissible, the Lax conditions for classical Riemann Problems presented, for example, in [13], are applied.

Therein, \mathbf{C}^0 is the set of continuous functions, \mathbf{BV} is the set of functions with bounded variations, \mathbf{C}_c^1 is the set of functions that are continuously differentiable with compact support and $B(\bar{w}, \bar{\delta})$ is the ball in \mathbb{R}^n centered at \bar{w} with radius $\bar{\delta}$.

Consider now the following coupling conditions conserving the flux in all three components across the pipe-to-pipe intersection:

$$(25) \quad \Psi(w^-; w^+) = \begin{bmatrix} M(w^+) - M(w^-) \\ N(w^+) - N(w^-) \\ P(w^+) - P(w^-) \end{bmatrix}.$$

This amounts to the conservation of mass of each phase and the equality of the dynamic pressure at the junction.

It can be shown that using (25) a solution in the sense of Definition 3.1 is equivalent to having a classical Riemann problem on \mathbb{R} with initial data in a neighborhood of a subsonic state \bar{w} . In this sense, Ψ given by (25) is therefore the obvious choice. This function can be extended to a coupling condition for $m + p$ connected pipes as shown in Remark 3.1.

In the following, we discuss the procedure for obtaining states at a general junction with $m + p$ connected pipes such that the coupling conditions of Remark 3.1 are fulfilled.

Consider an intersection of $m + p$ pipes with $i \in \{1, \dots, m\}$ incoming and $i \in \{m + 1, \dots, m + p\}$ outgoing pipes. Assume we have a state $\bar{w} = (\bar{w}^+, \bar{w}^-) \in A_0$ such that $\bar{w}_{m+p} \in \tilde{A}_0$ (as defined in (21)). Further, assume that the coupling conditions are fulfilled, i.e., $\Psi(\bar{w}^-; \bar{w}^+) = 0$. In order to obtain a well-posed problem, we need to ensure that for states w in a (possibly small) neighborhood of \bar{w} the coupling conditions are satisfied. The construction presented in [11] which relies on the implicit function theorem is adopted. It proceeds as follows: Consider a state $w = (w^-, w^+)$ such that $w_i^- \in A_0$ for $i = 1, \dots, m$ and $w_i^+ \in A_0$ for $i = m + 1, \dots, m + p - 1$ and $w_{m+p}^+ \in \tilde{A}_0$ and such that w is sufficiently close to \bar{w} . Consider the problem of determining a solution $(\vec{\xi}, \eta) = (\xi_1, \dots, \xi_{m+p}, \eta)$ to

$$(26) \quad \begin{aligned} &\Psi(L_1^-(\xi_1, w_1^-), \dots, L_1^-(\xi_m, w_m^-), L_3^+(\xi_{m+1}, w_{m+1}^+), \dots, \\ &\quad L_3^+(\xi_{m+p-1}, w_{m+p-1}^+), L_3^+(\xi_{m+p}, L_2(\eta, w_{m+p}^+)) = 0. \end{aligned}$$

If $\Psi \in C^1$ in its respective arguments and if the determinant of the derivative of Ψ with respect to $(\vec{\xi}, \eta)$ at $\vec{\xi} = 1, \eta = 1$ and for $w = \bar{w}$ is non-zero, then there exists a small neighborhood $B_\delta(\bar{w})$ such that problem (26) admits a unique solution $(\vec{\xi}^*, \eta^*)$. Furthermore, let the state \hat{w} be given by

$$(27a) \quad \hat{w}_i = L_1^-(\xi_i^*, w_i^-), \quad i = 1, \dots, m,$$

$$(27b) \quad \hat{w}_i = L_3^+(\xi_i^*, w_i^+), \quad i \in \{m + 1, \dots, m + p - 1\},$$

$$(27c) \quad \hat{w}_{m+p} = L_3^+(\xi_{m+p}^*, L_2(\eta^*, w_{m+p}^+)).$$

Then, the state \hat{w} fulfills the coupling condition

$$\Psi(\hat{w}) = 0.$$

Other results in this direction have been proved in [2, 6] for the case of isothermal Euler equations and in [12, 17] for the case of the Euler equations. Moreover, for the case of the Riemann problem at the junction, the "additivity" property is preserved just as for the standard Lax Riemann solver [7, 13], i.e., if (w^-, w^o) and (w^o, w^+) are Riemann data for a stationary solution of the Riemann problem at the junction, then so is (w^-, w^+) .

Remark 3.1. *Let us consider a junction with m ingoing pipes with the flow variables in those pipes denoted by w_1, \dots, w_m and p outgoing pipes with the flow variables denoted by w_{m+1}, \dots, w_{m+p} . One*

example of the coupling condition map here is given by

$$\Psi(w_1, \dots, w_m, w_{m+1}, \dots, w_{m+p}) = \begin{pmatrix} \sum_{i=1}^m M(w_i(t, 0-)) = \sum_{i=1}^p M(w_{m+i}(t, 0+)) \\ \sum_{i=1}^m N(w_i(t, 0-)) = \sum_{i=1}^p N(w_{m+i}(t, 0+)) \\ P(w_1(t, 0-)) = P(w_2(t, 0-)) \\ \vdots \\ P(w_{m-1}(t, 0-)) = P(w_m(t, 0-)) \\ P(w_m(t, 0-)) = P(w_{m+1}(t, 0+)) \\ P(w_{m+1}(t, 0+)) = P(w_{m+2}(t, 0+)) \\ \vdots \\ P(w_{m+p-1}(t, 0+)) = P(w_{m+p}(t, 0+)) \end{pmatrix}.$$

The first two rows of Ψ are compulsory. They express the conservation of mass of each phase at the junction. The last $m + p - 1$ rows of Ψ express the equality of the dynamic pressure at the junction. Similar conditions have been proposed in [2, 6, 7]. Some other conditions used in the literature include the equality of the pressure at the junction. For the p-system, many other conditions were proposed and compared in [8]. Similarly, other conditions can be envisioned for the case of more than one connected pipe. However, it is so far unclear which of the other possible conditions are reasonable. To this end, further investigations and experiments might have to be conducted. We leave the discussion of other conditions as well as their validation for future work.

A numerical scheme has, at any given point in time, to produce boundary values for each connected pipe given the current state in the pipe and the function Ψ . Assume the current state at the pipe intersection is $w_{0,i}^-$ for $i \in \{1, \dots, m\}$ pipes connected at $x = 0$ and incoming to the intersection and $w_{0,i}^+$ for $i \in \{m + 1, \dots, m + p\}$ pipes connected at $x = 0$ and being outgoing to the intersection. In order to advance a given finite volume scheme to the next time level, we need (at least first-order) boundary conditions at $x = 0$ for both incoming and outgoing pipes. To obtain the boundary values \hat{w}_i^\pm for $i \in \{1, \dots, m + p\}$ for each pipe, we solve for $(\vec{\xi}, \eta) = (\xi_1, \dots, \xi_m, \xi_{m+1}, \dots, \xi_{m+p-1}, \xi_{m+p}, \eta)$ the equation (26). Clearly, this function is highly nonlinear in $(\vec{\xi}, \eta)$ and may be solved by a Newton's method starting from $(\vec{0}, 0)$. Provided we have a solution $(\vec{\xi}^*, \eta^*)$ the boundary conditions for each pipe are given by equation (27).

In general, equation (26) has to be computed at every time-step. If now the curves L_i^\pm are not explicit as in the case of a general pressure law, the computational effort in solving problem (26) can be large. It turns out that this is generally the case when the pressure law for the drift-flux model is nonlinear, since the integration of the differential equation describing the rarefaction curve in $L_{1,3}$ is not trivial. Therefore, the application of linearized Lax curves is proposed. Recall that the Lax curves through a given state \bar{w} are given as in Equation (15), for example, by

$$(28) \quad L_i(\xi; \bar{w}) = \begin{cases} S_i(\xi; \bar{w}), & \xi \geq 1 \\ R_i(\xi; \bar{w}), & \xi < 1 \end{cases}$$

where $\xi \mapsto S_i(\xi; \bar{w})$ and $\xi \mapsto R_i(\xi; \bar{w})$ are the i -shock and the i -rarefaction curves through w , respectively. With the parameterization of these curves, they have a tangency of second order at the point w , i.e.

$$(29) \quad R_i(\xi; \bar{w}) - S_i(\xi; \bar{w}) = \mathcal{O}(\xi^3).$$

Hence, the composite function, $L_i(\xi; \bar{w})$ in (28) is smooth for $\xi \neq 1$, and twice continuously differentiable at $\xi = 1$. Moreover, its second derivatives are Lipschitz-continuous functions of ξ and \bar{w} , see

[5]. A Taylor expansion of $L_i(\xi; \bar{w})$ about $\xi = 1$ given as

$$(30) \quad \tilde{L}_i(\xi; \bar{w}) = \bar{w} + (\xi - 1)r_i(\bar{w}) + \mathcal{O}((\xi - 1)^2),$$

where $r_i(\bar{w})$ are the eigenvectors given in (6) can be employed. In the numerical simulations below, we now use the linearized Lax-curves to obtain the boundary conditions (27). To be more precise, we replace the (correct) computation (26) by

$$(31) \quad \Psi \left(\tilde{L}_1^-(\xi_1, w_{0,1}^-), \dots, \tilde{L}_1^-(\xi_m, w_{0,m}^-), \tilde{L}_3^+(\xi_{m+1}, w_{0,m+1}^+), \dots, \right. \\ \left. \tilde{L}_3^+(\xi_{m+p-1}, w_{0,m+p-1}^+), \tilde{L}_3^+(\xi_{m+p}, \tilde{L}_2(\eta, w_{0,m+p}^+)) \right) = 0$$

and similarly for \hat{w}_i , i.e., for the solution $(\bar{\xi}^*, \eta^*)$ to (31), we set

$$(32a) \quad \hat{w}_i = \tilde{L}_1^-(\xi_i^*, w_{0,i}^-), i \in \{1, \dots, m\},$$

$$(32b) \quad \hat{w}_i = \tilde{L}_3^+(\xi_i^*, w_{0,i}^+), i \in \{m+1, \dots, m+p-1\} \text{ and } \hat{w}_{m+p} = \tilde{L}_3^+(\xi_{m+p}^*, L_2(\eta^*, w_{0,m+p}^+)).$$

It is expected that in the subsonic flow region the state does not change drastically from one timestep to the next. Therefore, the linearized Lax-curves are supposed to be close to the nonlinear ones. Therefore, also the boundary values \hat{w}_i obtained from (32) are close to (27). This is confirmed by the numerical simulations below.

4. NUMERICAL SIMULATIONS AND RESULTS

The numerical integration of the multiphase fluid flow model defined in (5) is done with a second-order relaxed scheme [20]. In all this section, one assumes, in general, that the pipes have a constant cross-section and the sound speed, unless stated otherwise, for phase 1 is taken as $a_1^2 = 16.0$ and for phase 2, $a_2^2 = 1.0$. Initial conditions are usually some perturbation of some stationary solutions. Newton's method is used to solve the system in equation (25) combined with the Lax curves as described in the proof of Proposition 3.1 in [3]. The proof gives the boundary conditions at the internal nodes of the network at the junction. This ensures that at every time step, the coupling conditions at the junction are satisfied. For the external (inlet to network or outlet from network) boundary conditions, the transparent boundary conditions [23] are used. For time integration, a second-order Runge-Kutta scheme with the strong-stability preserving (SSP) [16] property is used. The time step size is given dynamically by

$$\Delta t = \frac{0.75\Delta x}{\max(\varrho(\partial f(W)/\partial W))}$$

where the maximum is taken over all computational grid-points. Also take note that Δx is the spatial step-width and $\varrho(\partial f(W)/\partial W)$ is the spectral radius of the Jacobian of the flux function $f(W)$ with respect to the conserved variables, W .

In the following, a discussion of the numerical aspects of the coupling conditions are undertaken. To start with, a case of two connected pipes is considered. The aim here is to evaluate the solution provided by the coupling condition in comparison to the solutions obtained by solving a standard Riemann problem in a single pipe divided into two parts initially. Firstly a case with linear pressure with $\gamma = 1$ is investigated. This is the case where Lax curves can be obtained analytically, in general. The aim of this example is to compare the results of the exact expressions of Lax curves and the linearized curves. Secondly, the effect of sound speed is investigated culminating with the investigation of cases with nonlinear pressure as well as a small network.

4.1. Two connected pipes and the standard Riemann problem. This section serves to verify the qualitative behavior of the coupling conditions and to validate the use of the linearized Lax curves for a junction connecting two pipes. To achieve that goal, the isothermal pressure law which is the same as the isentropic pressure law (3) for $\gamma = 1$ is considered. Independently, the standard Riemann problem, the Riemann problem at the junction with two horizontal pipes and with the exact Lax curves and then with the linearized Lax curves is solved. It is expected that the three results will agree. The choice of the isothermal pressure law for this test is motivated by the fact that the exact expressions for the Lax curves can be determined. Here the Riemann data

$$(33) \quad w_l = (1.4712300, 2.2832400, 3.2928117), \quad w_r = (0.8070800, 1.2525284, 2.2928117)$$

are considered.

For the Riemann problem at the junction, $w^- = w_l$ and $w^+ = w_r$ are considered as the data in each pipe such that the conditions of Proposition 3.1 in [3] are satisfied. The mesh size of $N = 400$ was employed on a single pipe on which the standard Riemann solver was applied. For the Riemann problem at the junction, the mesh size of $N = 200$ was applied in each pipe. The results computed at time $t = 0.05$ for the standard Riemann, the Riemann problem at the junction with the exact Lax curves and the linearized Lax curves are presented in Figure 1.

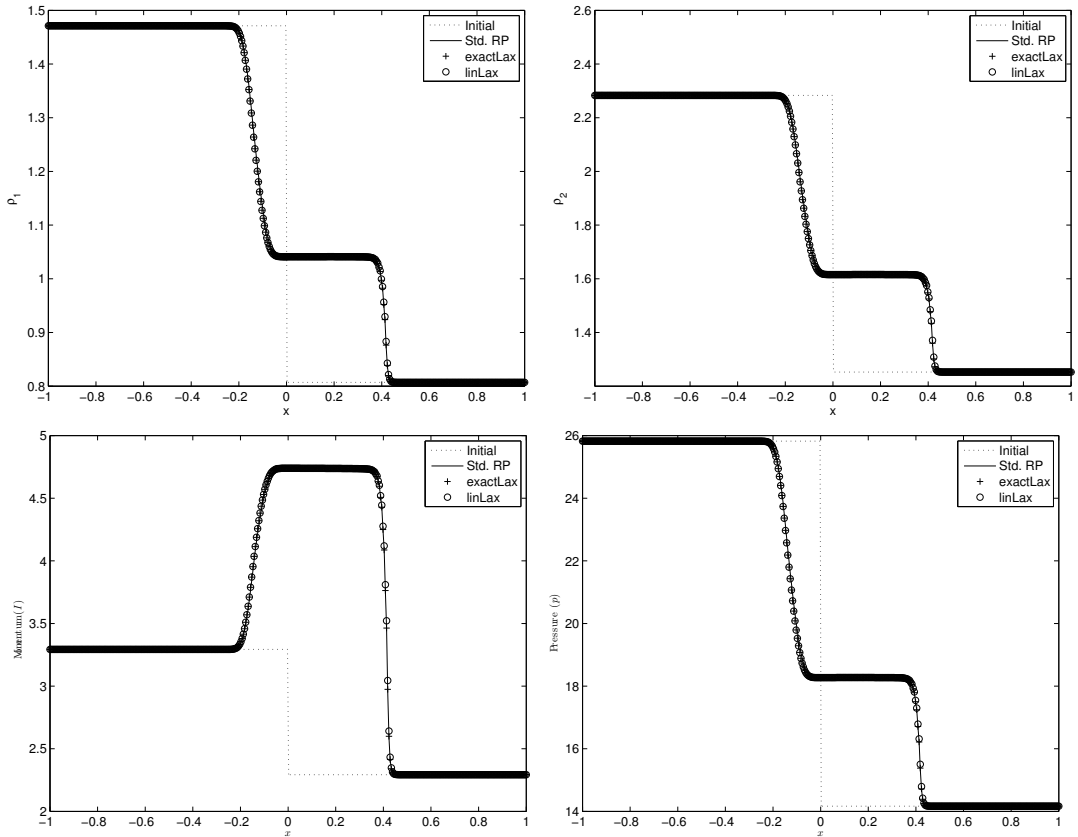


FIGURE 1. Profiles of the densities ρ_1 and ρ_2 , the momentum I , the common pressure p for the standard Riemann problem (continuous line), the Riemann problem at the junction with the use of the exact Lax curves (crosses) and the linearized Lax curves (circles).

There is qualitatively and quantitatively very good agreement between the two results as seen in the L^2 and L^1 errors on the momentum I and the pressure p presented in Table 1. In the table,

r^{RP} is the quantity r computed as the solution of the standard Riemann problem and r^{CP} be the same quantity computed as the solution of the Riemann problem at the junction of two coupled pipes.

Mesh size (N)	$\ I^{RP} - I^{CP}\ _{L^2}$	$\ p^{RP} - p^{CP}\ _{L^2}$	$\ I^{RP} - I^{CP}\ _{L^1}$	$\ p^{RP} - p^{CP}\ _{L^1}$
100	1.6339e-06	1.8844e-06	0.0012	0.0017
200	3.7917e-07	2.7096e-07	5.9362e-04	5.3481e-04
400	8.5111e-08	5.1969e-08	3.0193e-04	2.9461e-04

TABLE 1. L^2 error in the momemtum and pressure for the solution of the standard Riemann problem and the Riemann problem at the junction

This demonstrates two issues. Firstly, that qualitatively the solution of the Riemann problem at the junction with the coupling conditions proposed here is as accurate as the solution of the Sod shock tube problem solved directly. Secondly, that the linearization of the Lax curves is a good approximation for the solution of the Riemann problem at the junction.

Now an example with the isentropic pressure law given in Equation (3) is considered. Here $\gamma = 5/3$ is used and the following data

$$(34) \quad w_1 = (1.81832, 1.44174, -0.751082), \quad w_2 = (2.01667, 1.22004, -1.584711)$$

which is taken from [4] is used as the initial condition. The results are presented in Figure 2.

Again the results for the solution of the standard Riemann problem and the coupled pipes are in good agreement, see Table 2 where the errors are presented. In the table, r^{CPL} is the quantity r computed as the solution of the Riemann problem at the junction with the use of the linearised Lax curve and r^{CP} is as above.

Mesh size (N)	$\ I^{CP} - I^{CPL}\ _{L^2}$	$\ p^{CP} - p^{CPL}\ _{L^2}$	$\ I^{CP} - I^{CPL}\ _{L^1}$	$\ p^{CP} - p^{CPL}\ _{L^1}$
100	1.2886e-05	5.4828e-06	0.0038	0.0035
200	3.0500e-06	1.2959e-06	0.0011	0.0011
400	1.0113e-06	4.3049e-07	0.0012	0.0017

TABLE 2. L^2 error in the momemtum and pressure for the solution of the Riemann problem at the junction with exact Lax curves and linearised Lax curves computed for the problem in example 1

It can be observed that the shock and rarefaction waves are well resolved.

4.2. Effect of the sound speed on the flow. The case of a standard Riemann problem for the model equation (5) with the isentropic pressure law (3) and with $\gamma = 5/3$ is studied. The effect of changes in the compressibility factors of each phase on the multiphase model are investigated. The Riemann data is taken as

$$(35) \quad w(x, 0) = \begin{cases} (3.17123, 3.38324, 3.71816), & x < 0; \\ (2.70708, 4.0434, 3.5629), & x > 0. \end{cases}$$

The plots of the densities, the momentum and the pressure at time $t = 0.1$ are presented in Figure 3. The result for the case $a_2^2 = a_1^2$ compares well with those obtained in [4]. Also take note that the qualitative behavior of the solution for $a_1^2 < a_2^2$ is comparable to the case $a_1^2 = a_2^2$. Also, the flow is more compressive for $a_1^2 < a_2^2$.

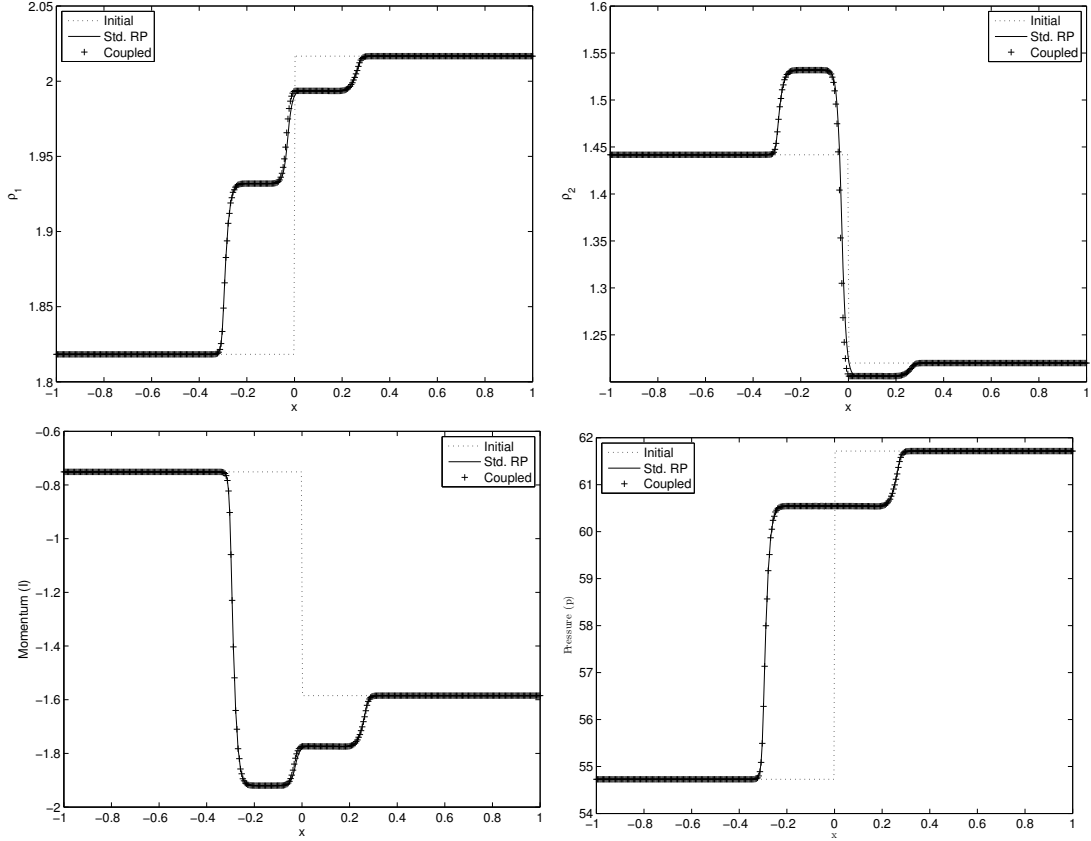


FIGURE 2. Profiles of the densities ρ_1 and ρ_2 , the momentum I , the common pressure p for the solution of standard Riemann problem (continuous line) and the Riemann problem at the junction with the use of the linearized Lax curves (crosses).

4.3. A junction with one ingoing and two outgoing pipes. In this section the nonlinear pressure law as given in (3) and a junction with three pipes with one incoming and two outgoing pipes is considered. For the numerical solution of the Riemann problem at the junction the linearization of the Lax curves described above is applied. The initial data in the pipes are taken as

$$(36) \quad \begin{aligned} w_1 &= (3.4500000, 2.4050000, 6.5056726); \\ w_2 &= (2.1300000, 4.1578000, 3.5720977); \\ w_3 &= (2.2534000, 2.4191412, 2.9335749). \end{aligned}$$

This data satisfy the coupling conditions and belong to the subsonic region (20). The results are presented in Figure 4 for the densities and pressure for times $0 \leq t \leq 0.08$. The dynamics are stable and one observes a wave moving backward in pipe 1 and waves moving forward in pipe 2 and pipe 3. Similar results were observed for the simulation of the isothermal Euler equation in [1, 2]. Therein, the coupling conditions map were combined with the demand and supply functions. Here the linearization of the Lax curves combined with the coupling conditions produce comparable results for the drift-flux model.

4.4. A network with five pipes and two junctions. We now implement the flow of the drift-flux model in a small network of five pipes with two junctions as shown in Figure 5. We, firstly, consider the linear pressure law given by $p = a_1\rho_1 + a_2\rho_2$ with $a_1 = 16$ and $a_2 = 1$. The initial conditions in

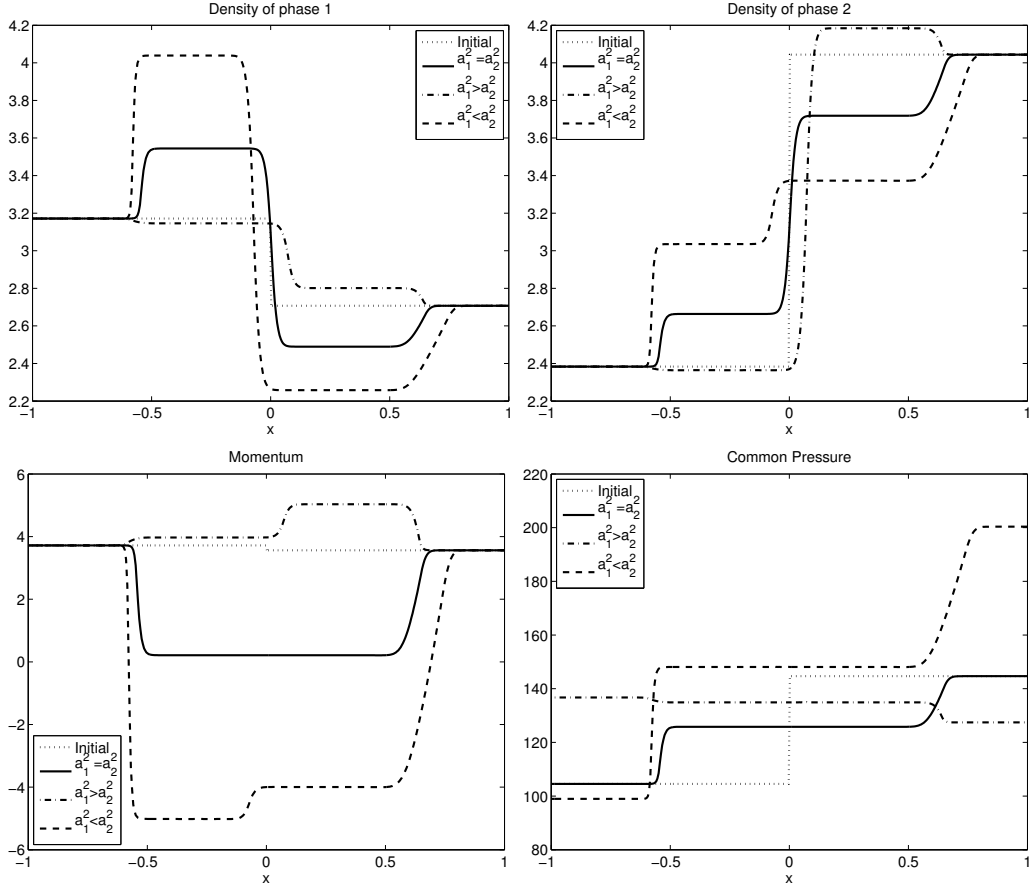


FIGURE 3. Profiles of the densities, ρ_1 , ρ_2 , in the first row, the momentum, I , and the pressure, p , for the Riemann problem for the drift flux model with different compressibility factors plotted at time $t = 0.1$. Here $a_1^2 = 1$ and $a_2^2 = 16$ and the other way around.

the pipes are given as

$$\begin{aligned}
 w_1 &= (6.4500, 12.8050, 31.9713); \\
 w_2 &= (10.3300, 3.3578, 2.4903); \\
 w_3 &= (1.9534, 4.5682, 29.4810); \\
 w_4 &= (9.0330, 18.3578, 13.0370); \\
 w_5 &= (0.4644, 1.2210, 16.4441).
 \end{aligned}$$

In Figure 6 the density and pressure in Pipe 1, Pipe 3 and Pipe 5 computed up to time $T = 0.10$ are presented. It can be observed that the flow at the junctions is well coupled and well resolved in the simulation. This indicates that the linearized model can be used to compute larger networks. The density, momentum and pressure in the horizontal pipes is also presented in Figure 7 – 8 to further demonstrate the above declaration.

In the next test example, we consider the pressure law given by $p(\rho_1, \rho_2) = (\rho_1 a_1^{2/\gamma} + \rho_2 a_2^{2/\gamma})^\gamma$ with $a_1 = 16$ and $a_2 = 1$ and $\gamma = 5/3$. The initial conditions in the pipes are given as

$$\begin{aligned}
 w_1 &= (1.1534, 0.9613, 9.4722254); \\
 w_2 &= (1.7798, 3.1579, 1.6480719); \\
 w_3 &= (1.6845000, 1.1980376, 7.8241535); \\
 w_4 &= (1.4585, 4.8579, -1.8018); \\
 w_5 &= (1.1845, 1.1012, 9.6260).
 \end{aligned}$$

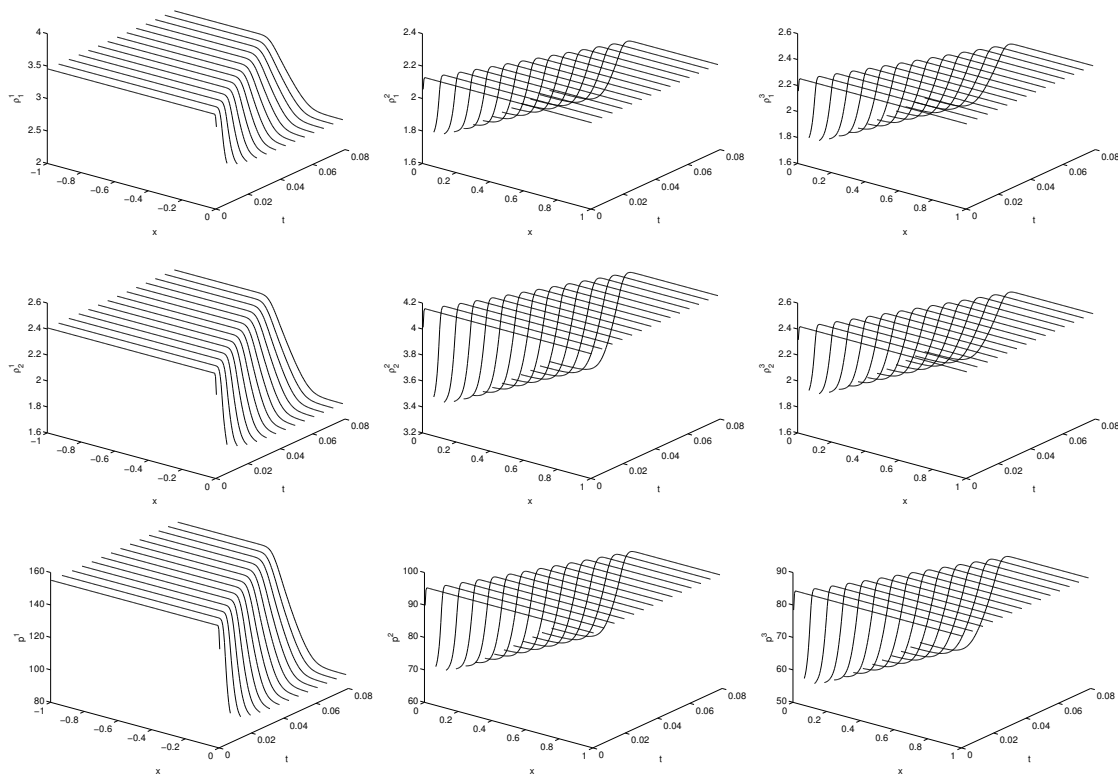


FIGURE 4. Snapshots of the density and pressure for the solution of the Riemann problem at the junction with one ingoing and two outgoing pipes. The coupling conditions and the linearization of the Lax curves are used.

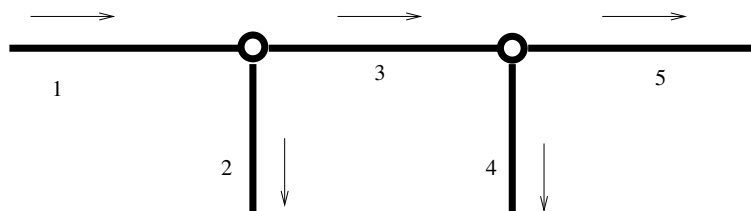


FIGURE 5. A small network with two junctions

The linearisation of the Lax curves and the coupling conditions are used to solve the Riemann problems at the junctions. The density and pressure for Pipe 1, Pipe 3 and Pipe 4 computed up to time $T = 0.10$ are presented in Figure 9. The flow at the junctions is well resolved by the simulation similar to the case in the previous example. Again, this is an indication that the model can indeed be applied for use in computing larger networks. Figures 10 – 11 demonstrate the quality of coupling of the density, the momentum and the pressure in the horizontal pipes at the final time.

5. SUMMARY AND FUTURE WORK

In this paper it has been demonstrated that the Riemann problem at the junction has a solution under some conditions on the initial data in each pipe. It has also been discussed that when the inflow is given and the coupling conditions are defined in a suitable way, one can always solve for the

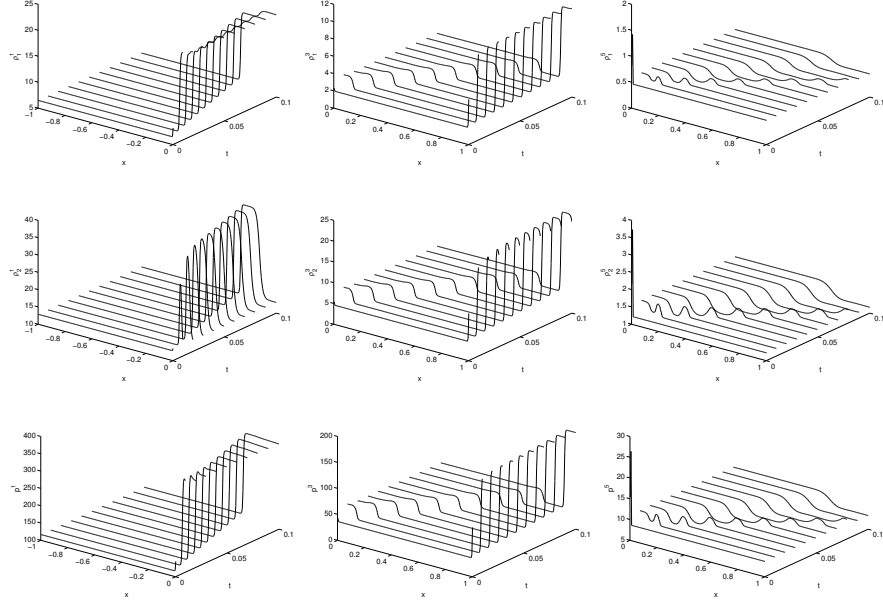


FIGURE 6. Snapshots of the density (top and middle row) and pressure (bottom row) in the three horizontal pipes (Pipe 1, 3 and 5) for the solution of the Riemann problem in a network of five pipes and two junctions.

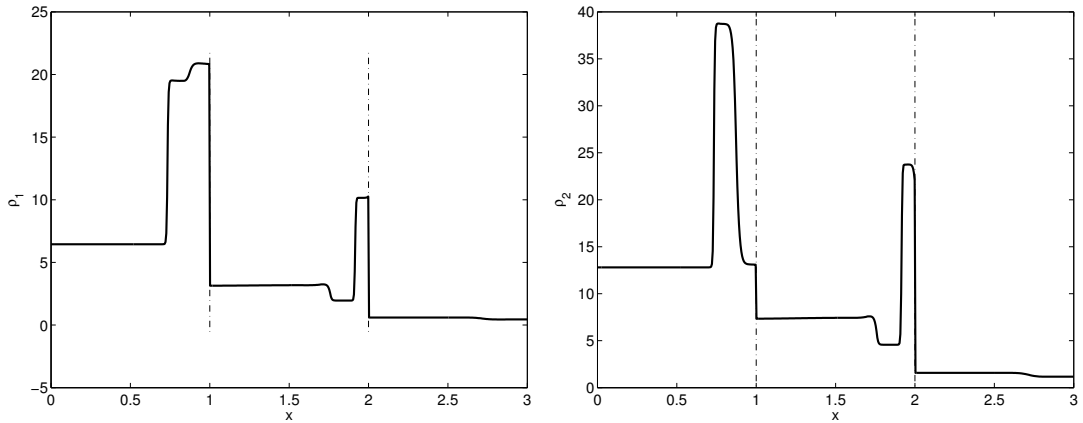


FIGURE 7. Densities of phase one and phase two in the horizontal pipes computed at time $T = 0.1$

outflow in the outgoing pipes. Numerical results that demonstrate that this approach is practical and its possible extension to more general networks have been presented.

Future work may comprise the solution of the Cauchy problems where the initial data do not need to be constant in each pipe. The existence of the solution in this case needs to be proven. As for single phase fluid, one might use the wave front tracking approach, see [10]. The difficulty here is that at any wave interaction, up to three waves can emerge and one needs to bound the strength of these waves accurately in order to obtain suitable estimates for the convergence of the front tracking algorithm.

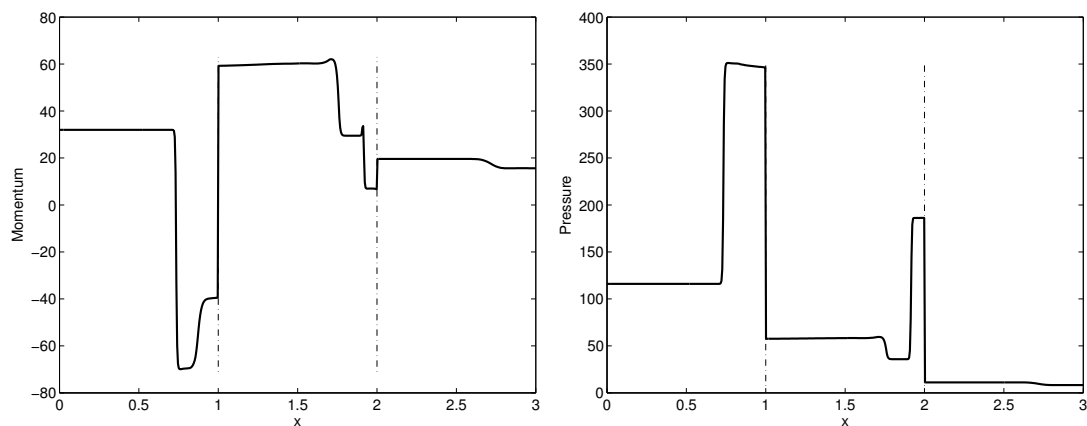


FIGURE 8. Momentum(I) and pressure(p) in the horizontal pipes computed at time $T = 0.1$

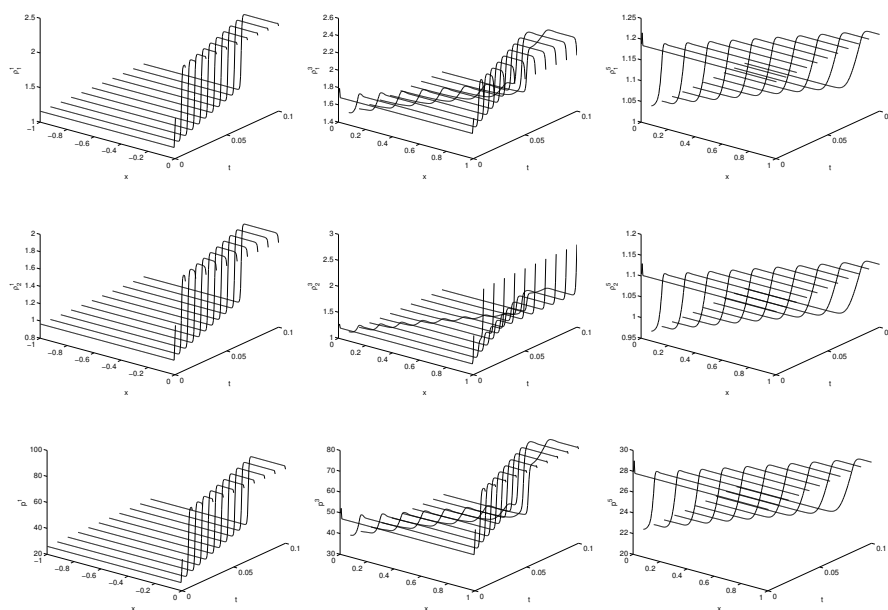


FIGURE 9. Snapshots of the densities (top and middle row) and pressure (bottom row) in the three horizontal pipes (Pipe 1, 3 and 5) for the solution of the Riemann problem in a network of five pipes and two junctions.

Acknowledgments:

The authors acknowledge fruitful suggestions from Prof. A. Kurganov of Tulane University. This work has been supported by DFG SPP 1253, HE5386/8-1 and HE5386/6-1, DAAD D/08/11076, 50727872, the Subcommittee B of Stellenbosch University and the Research Office of the University of KwaZulu-Natal. This work is also based on the research supported in part by the National Research Foundation (NRF) of South Africa UID: 74260, 85566. Part of this work was done when JMTN was visiting the University of Kaiserslautern.

REFERENCES

- [1] M. K. Banda, M. Herty, and A. Klar. Coupling conditions for gas networks governed by the isothermal Euler equations. *Networks and Heterogeneous media*, 1(2):295–314, June 2006.

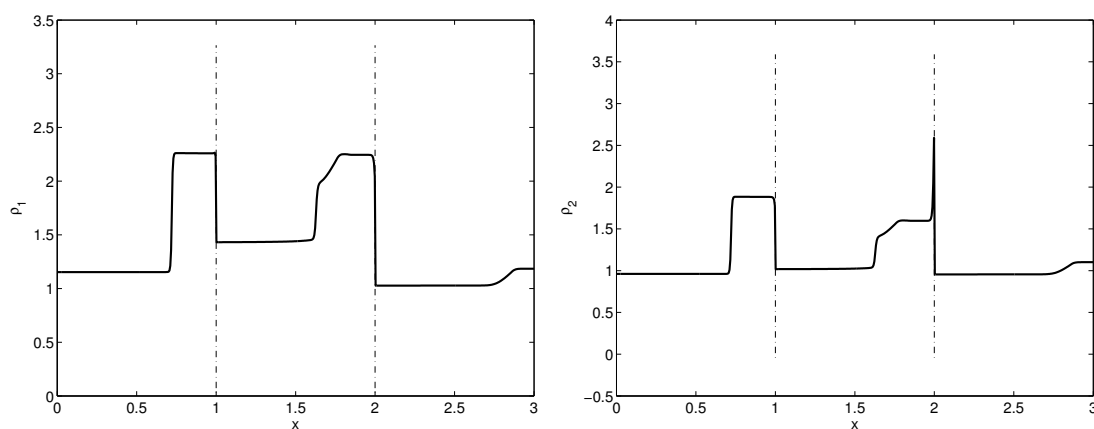


FIGURE 10. Densities of phase one and phase two in the horizontal pipes computed at time $T = 0.1$

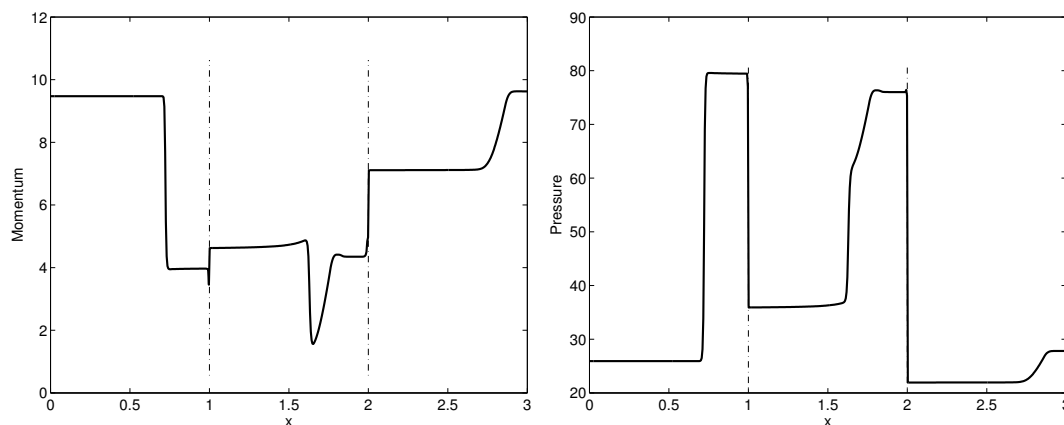


FIGURE 11. Momentum(I) and pressure(p) in the horizontal pipes computed at time $T = 0.1$

- [2] M. K. Banda, M. Herty, and A. Klar. Gas flow in pipeline networks. *Networks and Heterogeneous media*, 1(1):41–56, March 2006.
- [3] M. K. Banda, M. Herty, and J. M. T. Ngotchouye. Coupling the drift-flux models with unequal sonic speeds, *Math. and Comput. Appl.*, 15(4): 574–584, 2010.
- [4] M. K. Banda, M. Herty, and J. M. T. Ngotchouye. Towards a mathematical analysis of multiphase drift-flux model in networks. *SIAM J. Sci. Comp*, 31(6):4633–4653, 2010.
- [5] A. Bressan. *Hyperbolic systems of Conservation laws*, volume 20 of *Oxford Lectures Series in Mathematics and its Applications*. Oxford University Press, 2000.
- [6] R. M. Colombo and M. Garavello. A well posed Riemann problem for the p -system at a junction. *Networks and Heterogeneous Media*, 1(3):495–511, 2006.
- [7] R. M. Colombo and M. Garavello. On the Cauchy problem for the p -system at a junction. *SIAM Journal of Mathematical Analysis*, 39(5):1456–1471, 2008.
- [8] R. M. Colombo and M. Garavello. On the 1D modeling of fluid flowing through a junction, 2009. *ArXiv e-prints*, arXiv:0903.0781, 2009.
- [9] R. M. Colombo, G. Guerra, M. Herty, and V. Sachers. Modeling and optimal control of networks of pipes and canals. *SIAM J. Control Optim.*, 48(3):2032 – 2050, 2009.
- [10] R. M. Colombo, M. Herty, and V. Sachers. On 2×2 conservations laws at a junction. *SIAM Math. Anal.*, 40(2):605–622, 2008.
- [11] R. M. Colombo and F. Marcellini. Smooth and discontinuous junctions in the p -system. *Journal of Mathematical Analysis and Applications*, 361:440–456, 2010.
- [12] R. M. Colombo and C. Mauri. Euler system for compressible fluids at a junction. *Journal of Hyperbolic Differential equations*, 5(3):547–568, September 2008.

- [13] C. M. Dafermos. *Hyperbolic conservation laws in continuum physics*, volume 325 of *Grundlehren der mathematischen Wissenschaften*. Springer, 2 edition, 2005.
- [14] S. Evje and K. Fjelde. Relaxation schemes for calculation of two phase flow in pipes. *Math. and Comput. Modelling*, 36:535 - 567, 2002.
- [15] S. Evje and K. H. Karlsen. Global existence of weak solutions for a viscous two-phase model. *J. Differential Equations*, 245(9):2660–2703, 2008.
- [16] S. Gottlieb, C.-W. Shu, and E. Tadmor. Strongly stability preserving high-order time discretization methods. *SIAM rev.*, 43:89–112, 2001.
- [17] M. Herty. Coupling conditions for networked systems of Euler equations. *SIAM J. Sci. Comp.*, 30(3):1596–1612, 2007.
- [18] M. Herty and M. Seaid. Assessment of coupling conditions in water way intersections *Numerical Methods in Fluids*, 71(11):1438 – 1460, 2013.
- [19] M. Herty and M. Rascle. Coupling conditions for a class of second order models for traffic flow. *SIAM J. Math. Anal.*, 38(2):592–616, 2006.
- [20] S. Jin and Z. Xin. The relaxation schemes for systems of conservation laws in arbitrary space dimensions. *Comm. Pure Appl. Math.*, 48:235–276, 1995.
- [21] G. Leugering and E. J. P. G. Schmidt. On the modelling and stabilization of flows in networks of open canals. *SIAM J. Control Optim.*, 41(1):164–180, 2002.
- [22] R. J. LeVeque. *Numerical methods for conservation laws*. Birkhäuser Verlag, Basel, Switzerland, 1992.
- [23] R. J. LeVeque. *Finite volume methods for hyperbolic problems*. Cambridge texts in applied mathematics, Cambridge University Press, Cambridge, UK, 2002.
- [24] B. Piccoli and M. Garavello. *Traffic flow on networks*. Applied Math. Ser., American Institute of Mathematical Sciences.
- [25] G. Steinbach, S. Rademacher, P. Rentrop, and M. Schulz. Mechanism of coupling in river flow simulation systems. *J. of Comput. and Appl. Math.*, 168:459–470, 2004.

APPENDIX A. WAVE CURVES FOR A GENERALIZED PRESSURE

For completeness, the formulae for the equation of state that has been assumed in the article will be presented

$$\begin{aligned}
 p_1 &= \gamma a_1^{2/\gamma} (a_1^{2/\gamma} \rho_1 + a_2^{2/\gamma} \rho_2)^{\gamma-1}; \\
 p_2 &= \gamma a_2^{2/\gamma} (a_1^{2/\gamma} \rho_1 + a_2^{2/\gamma} \rho_2)^{\gamma-1}; \\
 p_{11} &= \gamma(\gamma - 1) a_1^{4/\gamma} (a_1^{2/\gamma} \rho_1 + a_2^{2/\gamma} \rho_2)^{\gamma-2}; \\
 p_{12} &= \gamma(\gamma - 1) a_1^{2/\gamma} a_2^{2/\gamma} (a_1^{2/\gamma} \rho_1 + a_2^{2/\gamma} \rho_2)^{\gamma-2}; \\
 p_{22} &= \gamma(\gamma - 1) a_2^{4/\gamma} (a_1^{2/\gamma} \rho_1 + a_2^{2/\gamma} \rho_2)^{\gamma-2}.
 \end{aligned}$$

If one takes $\gamma_1 \neq \gamma_2$ an equation for pressure of the form

$$a_1^{2/\gamma_1} \rho_1 p^{\frac{\gamma_1 - \gamma_2}{\gamma_1 \gamma_2}} - p^{1/\gamma_2} + a_2^{2/\gamma_2} \rho_2 = 0$$

is obtained. The partial derivatives needed for our discussion above can be presented implicitly using the following equations:

$$\begin{aligned}
& a_1^{2/\gamma_1} \left[p^{(\gamma_1 - \gamma_2)/(\gamma_1 \gamma_2)} + \left(\frac{\gamma_1 - \gamma_2}{\gamma_1 \gamma_2} \right) \rho_1 p^{(\gamma_1 - \gamma_2)/(\gamma_1 \gamma_2) - 1} p_1 \right] - \gamma_2^{-1} p^{1/\gamma_2 - 1} p_1 = 0; \\
& a_1^{2/\gamma_1} \left(\frac{\gamma_1 - \gamma_2}{\gamma_1 \gamma_2} \right) \rho_1^{(\gamma_1 - \gamma_2)/(\gamma_1 \gamma_2) - 1} p_2 - \gamma_2^{-1} p^{1/\gamma_2 - 1} p_2 + a_2^{2/\gamma_2} = 0; \\
& a_1^{2/\gamma_1} \left[\left(\frac{\gamma_1 - \gamma_2}{\gamma_1 \gamma_2} \right) p^{(\gamma_1 - \gamma_2)/(\gamma_1 \gamma_2) - 1} p_1 + \left(\frac{\gamma_1 - \gamma_2}{\gamma_1 \gamma_2} \right) \left\{ p^{(\gamma_1 - \gamma_2)/(\gamma_1 \gamma_2) - 1} p_1 + \right. \right. \\
& \left. \left. \left(\frac{\gamma_1 - \gamma_2}{\gamma_1 \gamma_2} - 1 \right) \rho_1 p^{(\gamma_1 - \gamma_2)/(\gamma_1 \gamma_2) - 2} p_1^2 + \rho_1 p^{(\gamma_1 - \gamma_2)/(\gamma_1 \gamma_2) - 1} p_{11} \right\} \right] \\
& - \gamma_2^{-1} \left((\gamma_2^{-1} - 1) p^{1/\gamma_2 - 2} p_1^2 + p^{1/\gamma_2 - 1} p_{11} \right) = 0; \\
& a_1^{2/\gamma_1} \left(\frac{\gamma_1 - \gamma_2}{\gamma_1 \gamma_2} \right) \left(\frac{\gamma_1 - \gamma_2}{\gamma_1 \gamma_2} - 1 \right) \rho_1 p^{((\gamma_1 - \gamma_2)/(\gamma_1 \gamma_2) - 2)} p_2^2 + \\
& p^{((\gamma_1 - \gamma_2)/(\gamma_1 \gamma_2) - 1)} p_{22} - \gamma_2^{-1} \left((\gamma_2^{-1} - 1) p^{1/\gamma_2 - 2} p_2 + p^{1/\gamma_2 - 1} p_{22} \right) = 0; \\
& a_1^{2/\gamma_1} \left(\frac{\gamma_1 - \gamma_2}{\gamma_1 \gamma_2} \right) \left[p^{((\gamma_1 - \gamma_2)/(\gamma_1 \gamma_2) - 1)} p_2 + \right. \\
& \left. \left(\frac{\gamma_1 - \gamma_2}{\gamma_1 \gamma_2} - 1 \right) \rho_1 p^{((\gamma_1 - \gamma_2)/(\gamma_1 \gamma_2) - 2)} p_1 p_2 + \rho_1 p^{((\gamma_1 - \gamma_2)/(\gamma_1 \gamma_2) - 1)} p_{12} \right] \\
& - \gamma_2^{-1} \left((\gamma_2^{-1} - 1) p^{1/\gamma_2 - 2} p_1 p_2 + p^{1/\gamma_2 - 1} p_{12} \right) = 0.
\end{aligned}$$

We briefly discuss the construction of the solution of the Riemann problem for our model with the pressure law given in (3) with $\gamma = 1$. To facilitate this discussion, we firstly quote a proposition without proof below [13]:

Proposition A.1. *We consider a Riemann Problem for (5) with initial data*

$$w(x, 0) = \begin{cases} w^- & \text{if } x < 0; \\ w^+ & \text{if } x > 0. \end{cases}$$

For $|w^+ - w^-|$ sufficiently small, there exists a unique weak self-similar solution to this Riemann problem with small total variation. This solution comprises four constant states $w_0 = w^-, w_1, w_2, w_3 = w^+$. When the i -th characteristic family is genuinely nonlinear w_i is joined to w_{i-1} by either an i -rarefaction wave or an i -shock, while when the i -characteristic family is linearly degenerate, w_i is joined to w_{i-1} by an i -contact discontinuity.

See also Figure 12 for an illustration.

We assume that the left state and right states w^- and w^+ are given and satisfy the conditions given in Proposition A.1. The states w_1 and w_2 are called intermediate states. We can then find ξ_1, ξ_2 and ξ_3 such that

$$(37) \quad w_1 = L_1^+(\xi_1; w^-), \quad \text{and} \quad w_2 = L_2(\xi_2; w_1), \quad \text{and} \quad w_2 = L_3^-(\xi_3; w^+).$$

For simplicity, we denote the momentum components of w_1 and w_2 as $I_1(\xi_1; w^-)$ and $I_3(\xi_3; w^+)$, respectively. The solution for the Riemann problem is found if we can solve for ξ_1, ξ_2 and ξ_3 the system

$$(38) \quad \begin{cases} \rho_1^+ \xi_3 & = \rho_1^- \xi_1 \xi_2, \\ \rho_2^+ \xi_3 & = \rho_2^- \xi_1 + \frac{a_2^2}{a_1^2} (1 - \xi_2) \rho_1^- \xi_1, \\ I_3(\xi_3; w^+) & = \frac{I_1(\xi_1; w^-)}{a_2^2 (\rho_1^- + \rho_2^-) \xi_1} \left((a_1^2 \rho_1^- + a_2^2 \rho_2^-) \xi_1 + (a_2^2 - a_1^2) \rho_1^- \xi_1 \xi_2 \right). \end{cases}$$

One can solve the first two equations in (38) and find ξ_2 and ξ_3 in terms of ξ_1 .

$$\xi_2 = \frac{\rho_1^+ p(\rho_1^-, \rho_2^-)}{\rho_1^- p(\rho_1^+, \rho_2^+)}, \quad \xi_3 = \frac{\rho_1^-}{\rho_1^+} \xi_1 \xi_2 = \frac{p(\rho_1^-, \rho_2^-)}{p(\rho_1^+, \rho_2^+)} \xi_1$$

One then replaces these expressions in the third equation in (38) and obtains a scalar equation to solve for ξ_1 . This equation is given by

$$I_3 \left(\frac{p(\rho_1^-, \rho_2^-)}{p(\rho_1^+, \rho_2^+)} \xi_1; w^+ \right) = \frac{I_1(\xi_1; w^-)}{a_2^2(\rho_1^- + \rho_2^-)} \left(p(\rho_1^-, \rho_2^-) + (a_2^2 - a_1^2) \rho_1^+ \frac{p(\rho_1^-, \rho_2^-)}{p(\rho_1^+, \rho_2^+)} \xi_1 \right).$$

If we assume for example that w_1 is connected to w^- with a 1-shock curve and that w_2 is connected to w^+ by a 3-rarefaction curve (see Figure 12),

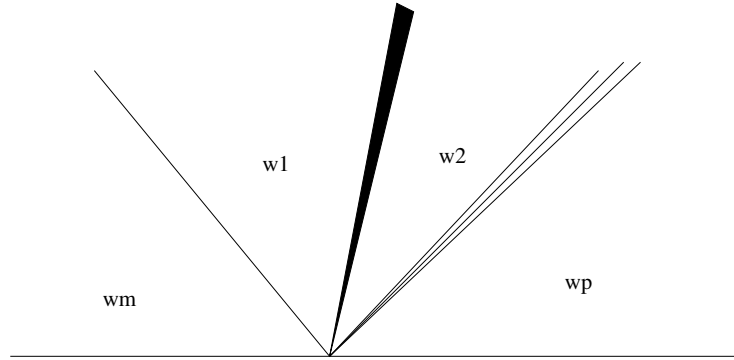


FIGURE 12. Wave structure for the solution of the Riemann problem for the Drift-flux model

we find that the map

$$g(\xi_1; w^-, w^+) = I_3 \left(\frac{p(\rho_1^-, \rho_2^-)}{p(\rho_1^+, \rho_2^+)} \xi_1; w^+ \right) - \frac{I_1(\xi_1; w^-)}{a_2^2(\rho_1^- + \rho_2^-)} \left(p(\rho_1^-, \rho_2^-) + (a_2^2 - a_1^2) \rho_1^+ \frac{p(\rho_1^-, \rho_2^-)}{p(\rho_1^+, \rho_2^+)} \xi_1 \right)$$

satisfy $g(1; w, w) = 0$ and $\frac{\partial g}{\partial \xi_1}(\xi_1, w^-, w^+) |_{(\xi_1=1, w, w)} \neq 0$ for some state w described below. Indeed, we have that

$$\frac{\partial g}{\partial \xi_1}(\xi_1, w^-, w^+) |_{(\xi_1=1, w, w)} = \frac{\rho_1 I}{\hat{\rho}} \left(\frac{a_1^2 - a_2^2}{a_2^2} \right) + 2\sqrt{a_1^2 \rho_1^2 + a_1^2 \rho_1 \rho_2 + a_2^2 \rho_2}.$$

The other cases corresponding to other waves structures in the solution are similar and are treated in the following result.

Proposition A.2. *Assume that we have a multi-phase fluid described with the equation of state (3) with a_1^2 and a_2^2 given. Let w be a state that satisfies the following condition*

$$(39) \quad \frac{\rho_1 I}{\hat{\rho}} \left(\frac{a_1^2 - a_2^2}{a_2^2} \right) + 2\sqrt{\hat{\rho}(\rho_1 p_1 + \rho_2 p_2)} \neq 0$$

Then, for w^- and w^+ close to w , the standard Riemann problem with data (w^-, w^+) admits a solution.